Viscoacoustic VTI and TTI wave equations and their application for anisotropic reverse time migration: Constant-Q approximation

Ali Fathalian and Kris Innanen

ABSTRACT

We investigated the simulation of Viscoacoustic wave propagation and reverse time migration (RTM) in transversely isotropic (TI) media, vertical TI (VTI) and tilted TI (TTI), within approximating constant-Q. Reverse time migration (RTM) is based on two-way wave equation and has advantages over than other imaging methods. Such wave propagation can be modeled with a finite difference scheme by introducing a series of standard linear solid (SLS) mechanisms, and it can be carried out within a computationally tractable region by making use of perfectly-matched layer (PML) boundary conditions. The Viscoacoustic wave equation for VTI and TTI mediums have been derived using the wave equation in anisotropic media by setting shear wave velocity as zero. Using the TI approximation and ignoring all spatial derivatives of the anisotropic symmetry axis direction leads to instabilities in some area of the model with the rapid variations in the symmetry axis direction. A solution to this problem is proposed that involves using a selective anisotropic parameter equating in the model to reduce the difference of Thompson parameters in areas of rapid changes in the symmetry axes. To eliminate the high-frequency instability problem, we applied the regularization operator and built a stable Viscoacoustic wave propagator in Ti media. After correcting for the effects of anisotropy and viscosity, the anisotropy RTM image in attenuation media with high resolution is obtained and compared with the isotropic RTM image.

INTRODUCTION

Attenuation is an increasingly indispensable component of wavefield simulation in seismic exploration and monitoring applications. It is a key element in many recent instances of data modeling, reverse time migration (RTM), and full waveform inversion (FWI). To consider the anisotropic media, the isotropic acoustic assumption for seismic processing and imaging method is not useful and affected the resolution and placed images of subsurface structures (Zhou et al., 2006a). Therefore, it is necessary to focus on the anisotropy and viscosity for complex media to obtain a significant improvement in image resolution and positioning. There are to way to consider the anisotropic medium, the pseudo-acoustic wave equation and the pure acoustic wave equation. Alkhalifah (1998, 2000) derived the pseudo-acoustic wave equation from the dispersion relation by setting the shear-wave velocity along the anisotropy symmetry axis to be zero. To reduce the computational time, based on pseudo-acoustic approximation, Zhou et al. (2006b) and Duveneck et al. (2008) developed and simplified the pseudo-acoustic wave equation into two coupled second- order partial differential equations to account for VTI media. Although the VTI wave equation is used to image structures which have similar properties with a VTI media (Crampin, 1984), but may not be satisfied in anisotropic dipping layers. The TTI equations have been derived from VTI equations by assuming the symmetry axis is non-vertical and locally variable (Fletcher et al., 2008; Zhang and Zhang, 2008). The TI wave equations with the

zero value of SV wave's velocity on the axis symmetry can't remove the effect of the residual shear wave, so the instability occurs. Fletcher et al. (2009) proposed the equations by adding non-zero S-wave velocity terms to solve the problem. To stabilize wave propagation and reduce shear wave artifacts the parameters models of anisotropy can be smoothing before numerical simulation, and setting $\varepsilon = \delta$ in the regions around source and areas with the high symmetry axis gradient (Zhang and Zhang, 2008; Yoon et al., 2010). However, to investigate the RTM images in anisotropic viscoelastic medium, generally, the focus is on the anisotropy or viscosity. In this work, we focus on both anisotropy and viscosity to obtain the accurate RTM images. In this paper, we investigate the simulation of wave propagation in anisotropic viscoacoustic medium within approximating constant-Q using a split-field PML equation in the time domain, and derive a viscoacoustic wave equation of VTI and TTI mediums. This article is organized as follows. In the first section we describe the background of research, and then the anisotropic model is presented, and we introduce the split-field PML formulation of the approximate constant-Q anisotropic viscoacoustic wave equation for VTI and TTI mediums in the second section. Numerical results on synthetic data are presented in the fourth section.

VISCOACOUSTIC WAVE EQUATION IN ANISOTROPIC MEDIA

In this section, we derive systems of first-order differential equations regarding the particle velocities and stresses that describe the propagation of waves in anisotropic media. The starting point for driving viscoacoustic wave equations is Hook's law, with the elastic tensor, together with the equation of motion in anisotropic media with $V_s = 0$ (Alkhalifah, 2000). We derive the viscoacoustic VTI equation directly from the acoustic VTI media and then the viscoacoustic TTI wave equations will calculate by introducing a rotation.

VISCOACOUSTIC VTI MEDIA EQUATION

In 2D case, the first order acoustic wave equations of VTI media is expressed as follow (Duveneck et al., 2008)

$$\begin{aligned} \sigma_H &= \rho V_P^2 \left[(1+2\varepsilon)\varepsilon_{11} + \sqrt{1+2\delta}\varepsilon_{33} \right], \\ \sigma_V &= \rho V_P^2 \left[\sqrt{1+2\delta}\varepsilon_{11} + \varepsilon_{33} \right], \end{aligned} \tag{1}$$

where σ_H and σ_V represent the horizontal and vertical stress components respectively. ε and δ are Thomsen parameters, and the $\varepsilon_{ij}$are the diagonal elements of strain tensor. The first order differential equations of acoustic VTI media can be obtained by taking a time derivative of stress-strain relationship given in eq.1 and combining the result with the equations of motion

$$\begin{aligned} \partial_t u_x &= (1/\rho)\partial_x \sigma_H, \\ \partial_t u_z &= (1/\rho)\partial_z \sigma_V, \end{aligned} \tag{2}$$

$$\begin{aligned} \partial_t \sigma_H &= \rho V_P^2 \left[(1+2\varepsilon)\partial_x u_x + \sqrt{1+2\delta}\partial_z u_z \right], \\ \partial_t \sigma_V &= \rho V_P^2 \left[\sqrt{1+2\delta}\partial_x u_x + \partial_z u_z \right], \end{aligned} \tag{3}$$

where $\partial_t \varepsilon_{ij} = \partial_{xi} u_i$ has been used, and u_x, and u_z are components of the particle velocity vector. Based on acoustic anisotropic medium, eq.2 and eq.3 can modify to extend an viscoacoustic anisotropic medium. The viscoacoustic wave equation in anisotropic media for a series of SLS can be written as

$$\begin{aligned} \partial_t u_x &= (1/\rho)\partial_x \sigma_H, \\ \partial_t u_z &= (1/\rho)\partial_z \sigma_V, \end{aligned} \tag{4}$$

$$\partial_t \sigma_H = \rho V_P^2 \left[(1+2\varepsilon) \left[\left[1 - \sum_{\ell=1}^{L} \left(1 - \frac{\tau_{\varepsilon\ell}}{\tau_{\sigma\ell}} \right) \right] \partial_x u_x - \sum_{\ell=1}^{L} r_{H\ell} \right] + \sqrt{1+2\delta}\partial_z u_z \right], \tag{5}$$

$$\partial_t \sigma_V = \rho V_P^2 \left[\sqrt{1+2\delta}\partial_x u_x + \left[1 - \sum_{\ell=1}^{L} \left(1 - \frac{\tau_{\varepsilon\ell}}{\tau_{\sigma\ell}} \right) \right] \partial_z u_z - \sum_{\ell=1}^{L} r_{V\ell} \right],$$

where $r_{H\ell}$, and $r_{V\ell}$, which are referred to as memory variables of horizontal and vertical stress components (Carcione et al., 1988), satisfy

$$\begin{aligned} \partial_t r_{H\ell} &= -\frac{1}{\tau_{\sigma\ell}} r_{H\ell} + \rho V_p^2 \left(\partial_x u_x \right) \frac{1}{\tau_{\sigma\ell}} \left(1 - \frac{\tau_{\varepsilon\ell}}{\tau_{\sigma\ell}} \right), \\ \partial_t r_{V\ell} &= -\frac{1}{\tau_{\sigma\ell}} r_{V\ell} + \rho V_p^2 \left(\partial_z u_z \right) \frac{1}{\tau_{\sigma\ell}} \left(1 - \frac{\tau_{\varepsilon\ell}}{\tau_{\sigma\ell}} \right) .1 \leq \ell \leq L, \end{aligned} \tag{6}$$

The stress and strain relaxation parameters, τ_ε and τ_σ, are related to the quality factor Q and the reference angular frequency ω as (Robertsson et al., 1994)

$$\begin{aligned} \tau_\sigma &= \frac{\sqrt{1+1/Q^2} - 1/Q}{\omega}, \\ \tau_\varepsilon &= \frac{1}{\omega^2 \tau_\sigma}. \end{aligned} \tag{7}$$

where ω is the central frequency of the source wavelet.

In order to introduce the PML boundary for such viscoacoustic waves, the first-order linear differential equations are modified using the complex coordinate stretching approach. In the frequency domain, derivative operators are replaced as follows

$$\begin{aligned} \partial_x &\rightarrow \left[1 + \frac{i d(x)}{\omega} \right] \partial_x, \\ \partial_z &\rightarrow \left[1 + \frac{i d(z)}{\omega} \right] \partial_z. \end{aligned} \tag{8}$$

By applying the complex coordinate stretching to the first-order linear differential equations 4, and 5 in the frequency domain we obtain

$$-i\omega \left[1 + \frac{d(x)}{-i\omega} \right] \tilde{u}_x = \frac{1}{\rho} \partial_x \tilde{\sigma_H}, \tag{9}$$

$$-i\omega\left[1+\frac{d(z)}{-i\omega}\right]\tilde{u}_z=-\frac{1}{\rho}\partial_z\tilde{\sigma_V}, \tag{10}$$

$$-i\omega\left[1+\frac{d(x)}{-i\omega}\right]\left[1+\frac{d(z)}{-i\omega}\right]\tilde{\sigma}_H=\rho V_P^2\left[(1+2\varepsilon)\left[\left[1-\sum_{\ell=1}^{L}\left(1-\frac{\tau_{\varepsilon\ell}}{\tau_{\sigma\ell}}\right)\right]\times\left(1+\frac{d(z)}{-i\omega}\right)\partial_x\tilde{u}_x-\sum_{\ell=1}^{L}r_{H\ell}\right]+\sqrt{1+2\delta}\left(1+\frac{d(x)}{-i\omega}\right)\partial_z\tilde{u}_z\right], \tag{11}$$

$$-i\omega\left[1+\frac{id(x)}{\omega}\right]\left[1+\frac{id(z)}{\omega}\right]\tilde{\sigma}_V=\rho V_P^2\left[\sqrt{1+2\delta}\left(1+\frac{d(z)}{-i\omega}\right)\partial_x\tilde{u}_x+\left[1-\sum_{\ell=1}^{L}\left(1-\frac{\tau_{\varepsilon\ell}}{\tau_{\sigma\ell}}\right)\right]\left(1+\frac{d(z)}{-i\omega}\right)\partial_z\tilde{u}_z-\sum_{\ell=1}^{L}r_{H\ell}\right], \tag{12}$$

where $\tilde{u}_x$, $\tilde{u}_z$,$\tilde{\sigma}_H$, and $\tilde{\sigma}_V$ are the temporal Fourier transforms of u_x, u_z, σ_H, and σ_V, respectively. To calculate the split-field PML formulations these equations must be transformed back to the time domain. In the split-field PML formulations, the velocity, and pressure fields are split into two independent parts based on the spatial derivative terms in the original equations in two space dimensions. For one relaxation mechanism (L = 1), which is sufficient for practical purposes (Blanch et al., 1995), equations 9, 10,11, and 12 are transformed back to time domain to get the split-field PML formulations

$$\partial_t u_x=\frac{1}{\rho}\partial_x\sigma_H-d(x)u_x, \tag{13}$$

$$\partial_t u_z=\frac{1}{\rho}\partial_z\sigma_V-d(z)u_z, \tag{14}$$

$$\partial_t\sigma_H=\rho V_P^2\left[(1+2\varepsilon)\left[\left(\frac{\tau_\varepsilon}{\tau_\sigma}\right)\left[\partial_x(u_x+d(z)u_x^{(1)})\right]-r_H\right]+\sqrt{1+2\delta}\left[\partial_z(u_z+d(x)u_z^{(1)})\right]\right]-(d(x)+d(z))\sigma_H-d(x)d(z)\sigma_H^{(1)}, \tag{15}$$

$$\partial_t\sigma_V=\rho V_P^2\left[\sqrt{1+2\delta}\left[\partial_x(u_x+d(z)u_x^{(1)})\right]+\left(\frac{\tau_\varepsilon}{\tau_\sigma}\right)\left[\partial_z(u_z+d(x)u_z^{(1)})\right]-r_V\right]-(d(x)+d(z))\sigma_V-d(x)d(z)\sigma_V^{(1)}, \tag{16}$$

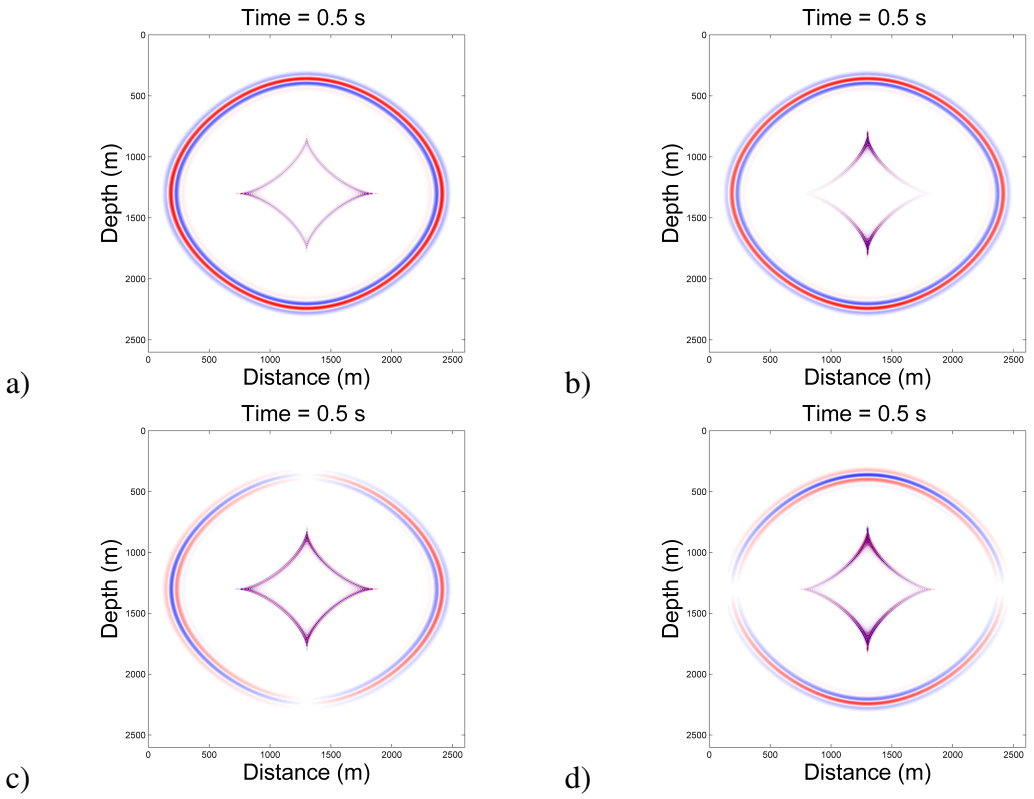

FIG. 1: 2D wavefield snapshots in a viscoacoustic VTI medium with $\varepsilon = 0.2$, and $\delta = 0.05$ a) σ_H, b) σ_V, c) u_x, and d) u_z. The shear wave artifacts are generated by source and have not been suppressed.

where the auxiliary variables $u_x^{(1)}$, $u_z^{(1)}$, $\sigma_H^{(1)}$, and $\sigma_V^{(1)}$ are the time-integrated components for velocity, pressure and memory variable fields. When the seismic wave propagation, the high-frequency leads to instability. To avoid the high-frequency effect on reverse time propagation, the regularization must be considered. We construct a regularized equation based on equations 15, and 16 in viscoacostic VTI media

$$\partial_t \sigma_H = \rho V_P^2 \left[(1+2\varepsilon) \left[\left(\frac{\tau_\varepsilon}{\tau_\sigma} \right) \left[\partial_x (u_x + d(z) u_x^{(1)}) \right] - r_H \right] + \sqrt{1+2\delta} \left[\partial_z (u_z + d(x) u_z^{(1)}) \right] \right] - \left[\epsilon \rho V_P \sqrt{1+2\varepsilon} [\partial_t (u_x + d(z) u_x^{(1)})] \right] - (d(x) + d(z)) \sigma_H - d(x) d(z) \sigma_H^{(1)}, \quad (17)$$

$$\partial_t \sigma_V = \rho V_P^2 \left[\sqrt{1+2\delta} \left[\partial_x (u_x + d(z) u_x^{(1)}) \right] + \left(\frac{\tau_\varepsilon}{\tau_\sigma} \right) \left[\partial_z (u_z + d(x) u_z^{(1)}) \right] - r_V \right] - \left[\epsilon \rho V_P [\partial_t (u_z + d(x) u_z^{(1)})] \right] - (d(x) + d(z)) \sigma_V - d(x) d(z) \sigma_V^{(1)}. \quad (18)$$

where ϵ is a small positive regularization parameter.

We examine the numerical character of the solutions of the wave equation for viscoacoustic VTI media as created using the split-field PML boundary approach. We first

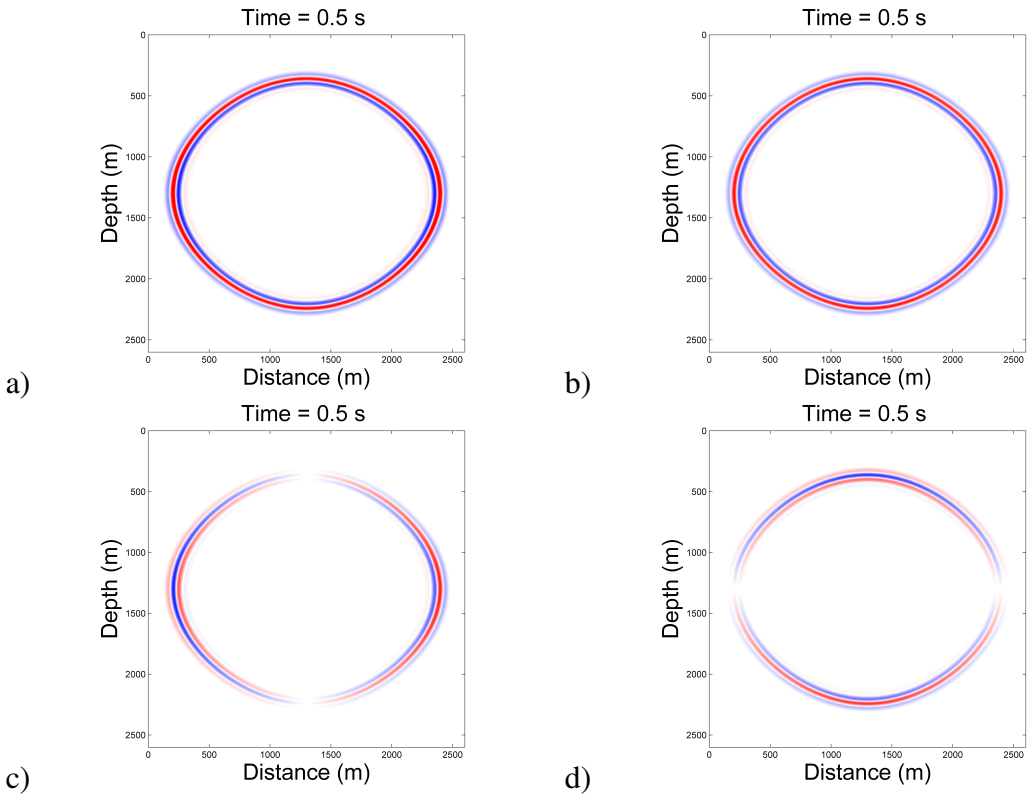

FIG. 2: 2D wavefield snapshots with suppression of source-generated shear wave artifacts.

consider propagation of waves in a homogeneous model. The anisotropic viscoacoustic medium considered here is characterized by the constant velocity model ,$V_P = 2500m/s$, where the size of the grid is 651×651. The source is located at the point (1300m, 1300m), and the source signature is a zero-phase Ricker wavelet with a central frequency of 25 Hz. The grid spacing in the x and z directions is 4m, and the Thomsen anisotropic parameters $\varepsilon = 0.2$ and $\delta = 0.05$. In Figure 1 the $0.5s$ snapshots of the 2D anisotropic viscoacoustic wavefield are plotted. The front wave of the P wave presents an elliptical shape because of anisotropic effect.

There is a problem due to shear wave that generated by the source (Figure 1), which for the acoustic and viscoacoustic medium have to regarded as artifacts(Alkhalifah, 2000; Grechka et al., 2004). The shear wave artifacts generated in an elliptic media ($\varepsilon \neq \delta$), and they can suppress at the source by design a small smoothly tapered circular region with $\varepsilon = \delta$ around the source(Figure 2). In Figure 2, there are only P waves and shear waves are suppressed.

However, the shear waves that generated by source don't consider as the problem when the source located in the isotropic part of the model. In Figure 3 we show the effect of attenuation on amplitude and phase of a propagating seismic wave in a inhomogeneous medium for different values of quality factor (Q=infinity, Q=100, Q=20 and Q=10). The attenuation affected the seismic wave energy, and the phase velocity of waves in all directions are inconsistent. In Figure 4 depth profiles of the wave field extracted at $t = 0.5s$ are plotted. The solid black line, solid blue line, dashed red line, and dashed black line

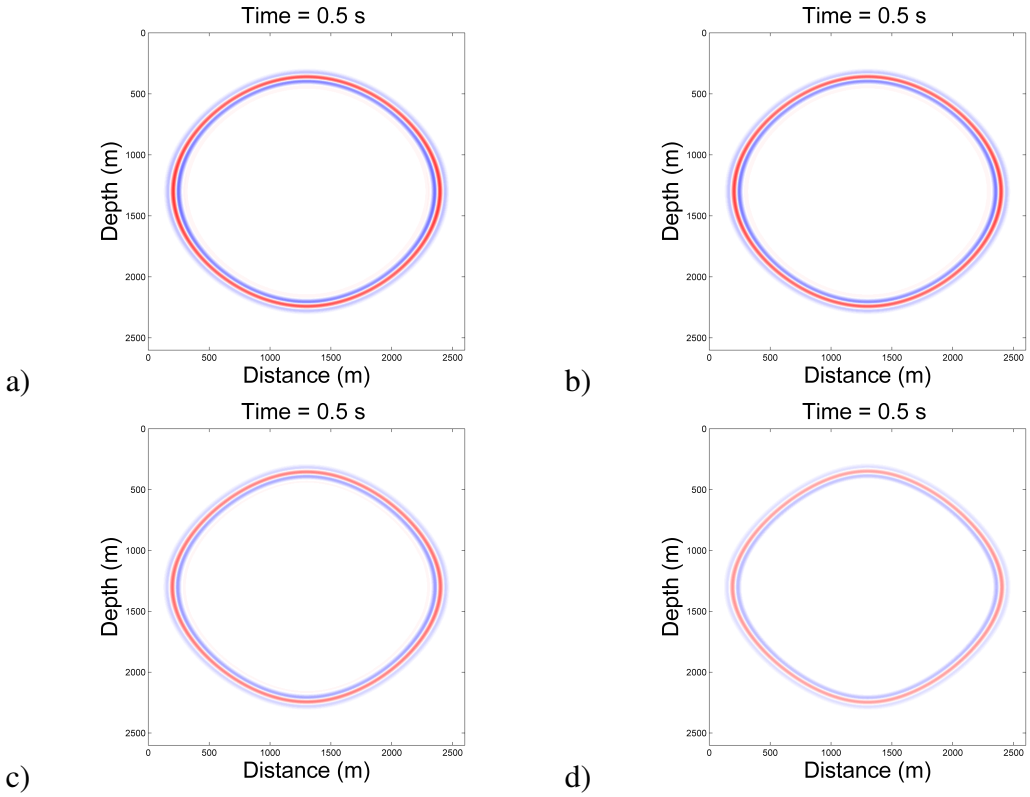

FIG. 3: The $0.5s$ snapshots with four different quality factors in a VTI medium: (a) $Q = infinity$, (b)$Q = 100$, (c) $Q = 20$, and (c) $Q = 10$.

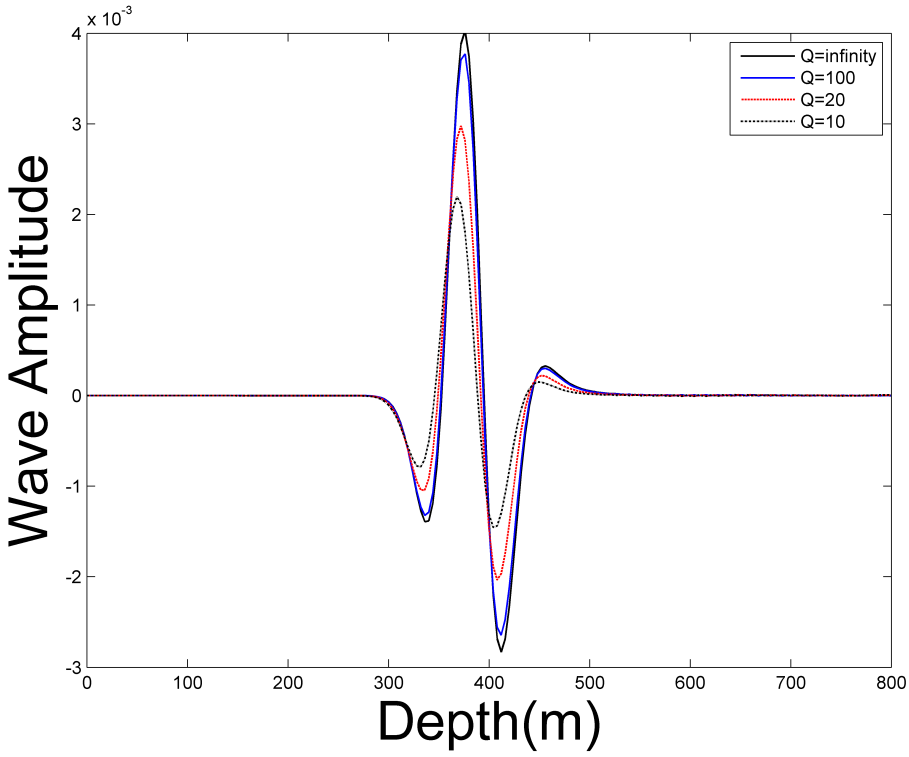

FIG. 4: Depth traces of FD showing the comparison trace number 370 of viscoacoustic VTI medium with different Q.

represent the acoustic wave, and three examples of the viscoacoustic wave, with $Q = 100$, $Q = 20$ and $Q = 10$ respectively. There are two main effects visible, reduced amplitude and phase shift due to dispersion. The phases do not match, and mismatch increases with the decrease of the Q value and the attenuation effect is more obvious.

VISCOACOUSTIC TTI MEDIA EQUATION

The one simplest and most practical approximations for anisotropic media is VTI medium, while is only valid for simple geologic formations. In anticline structures and thrust sheets where sediments are steeply dipping, the VTI medium approximation is not useful because of non-vertical symmetry axis of the medium. Therefor, to consider such as areas is better to use the tilted transversely isotropic (TTI) media. The one way to calculate the TTI equations is to locally rotate the coordinate system of VTI medium. The rotation matrix as function of the polar angle and azimuth angle is defined as

$$\mathbf{R} = \begin{pmatrix} \cos\theta\cos\varphi & \cos\theta\sin\varphi & -\sin\theta \\ -sin\varphi & cos\varphi & 0 \\ \sin\theta\cos\varphi & \sin\theta\sin\varphi & \cos\theta \end{pmatrix} \tag{19}$$

where θ represent the tilt angle and φ represent the azimuth of tilt for TTI symmetry axis. The spatial derivative in a rotated coordinate system can be written as

$$\begin{pmatrix} \partial_{x'} \\ \partial_{y'} \\ \partial_{z'} \end{pmatrix} = \mathbf{R} \begin{pmatrix} \partial_x \\ \partial_y \\ \partial_z \end{pmatrix} \tag{20}$$

where primed refer to the rotated coordinate system. Substituting eq.20 into eq.4 and eq.5, the 2D viscoacoustic wave equation in anisotropic TTI media for a series of SLS can be written as

$$\begin{aligned} \partial_t u_x &= (1/\rho)\partial_{x'}\sigma_H, \\ \partial_t u_z &= (1/\rho)\partial_{z'}\sigma_V, \end{aligned} \tag{21}$$

$$\begin{aligned} \partial_t \sigma_H &= \rho V_P^2 \left[(1+2\varepsilon) \left[\left[1 - \sum_{\ell=1}^{L} \left(1 - \frac{\tau_{\varepsilon\ell}}{\tau_{\sigma\ell}} \right) \right] \partial_{x'} u_x - \sum_{\ell=1}^{L} r_{H\ell} \right] + \sqrt{1+2\delta}\,\partial_{z'} u_z \right], \\ \partial_t \sigma_V &= \rho V_P^2 \left[\sqrt{1+2\delta}\,\partial_{x'} u_x + \left[1 - \sum_{\ell=1}^{L} \left(1 - \frac{\tau_{\varepsilon\ell}}{\tau_{\sigma\ell}} \right) \right] \partial_{z'} u_z - \sum_{\ell=1}^{L} r_{V\ell} \right], \end{aligned} \tag{22}$$

where $\partial_{x'}$, and $\partial_{z'}$ are the first order differential operators in the rotated coordinate system aligned with the symmetry axis:

$$\begin{aligned} \partial_{x'} &= \cos\theta\cos\varphi\partial_x - \sin\theta\partial_z, \\ \partial_{z'} &= \cos\varphi\sin\theta\partial_x + \cos\theta\partial_z, \end{aligned} \tag{23}$$

For one relaxation mechanism (L = 1), substituting eq.23 in the eq.21, and eq.22 and applying the complex coordinate stretching to the first-order linear differential equations in the frequency domain. To calculate the split-field PML formulations these equations transformed back to the time domain. The split-PML viscoacoustic wave equations in TTI medium become

$$\partial_t u_x = \frac{1}{\rho}(\cos\theta\cos\varphi\partial_x - \sin\theta\partial_z)\sigma_H - d(x)u_x, \tag{24}$$

$$\partial_t u_z = \frac{1}{\rho}(\cos\varphi\sin\theta\partial_x + \cos\theta\partial_z)\sigma_V - d(z)u_z, \tag{25}$$

$$\begin{aligned} \partial_t \sigma_H = \rho V_P^2 \Bigg[(1+2\varepsilon) \Bigg[\left(\frac{\tau_\varepsilon}{\tau_\sigma} \right) \left[(\cos\theta\cos\varphi\partial_x - \sin\theta\partial_z)(u_x + d(z)u_x^{(1)}) \right] - r_H \Bigg] \\ + \sqrt{1+2\delta} \left[(\cos\varphi\sin\theta\partial_x + \cos\theta\partial_z)(u_z + d(x)u_z^{(1)}) \right] \Bigg] \\ - (d(x)+d(z))\sigma_H - d(x)d(z)\sigma_H^{(1)}, \end{aligned} \tag{26}$$

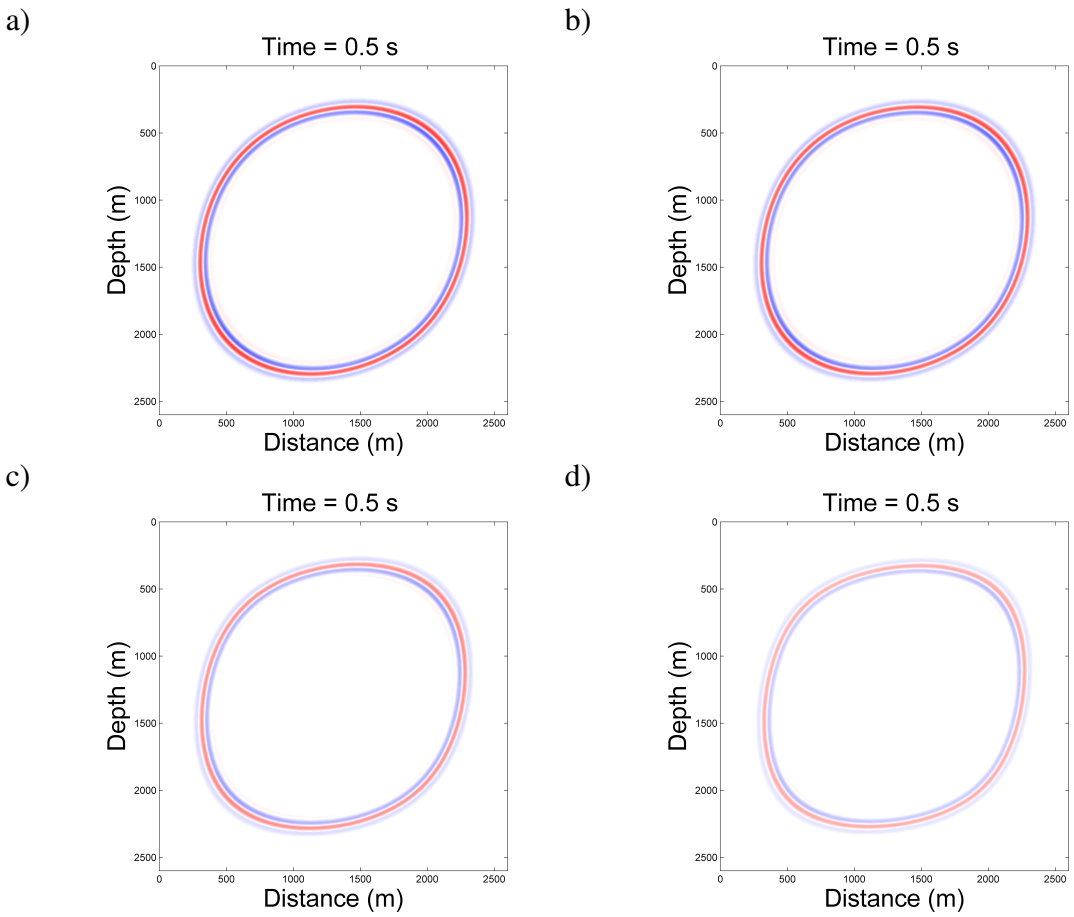

FIG. 5: The $0.5s$ snapshots with four different quality factors in a VTI medium: (a) $Q = infinity$, (b)$Q = 100$, (c) $Q = 20$, and (c) $Q = 10$.

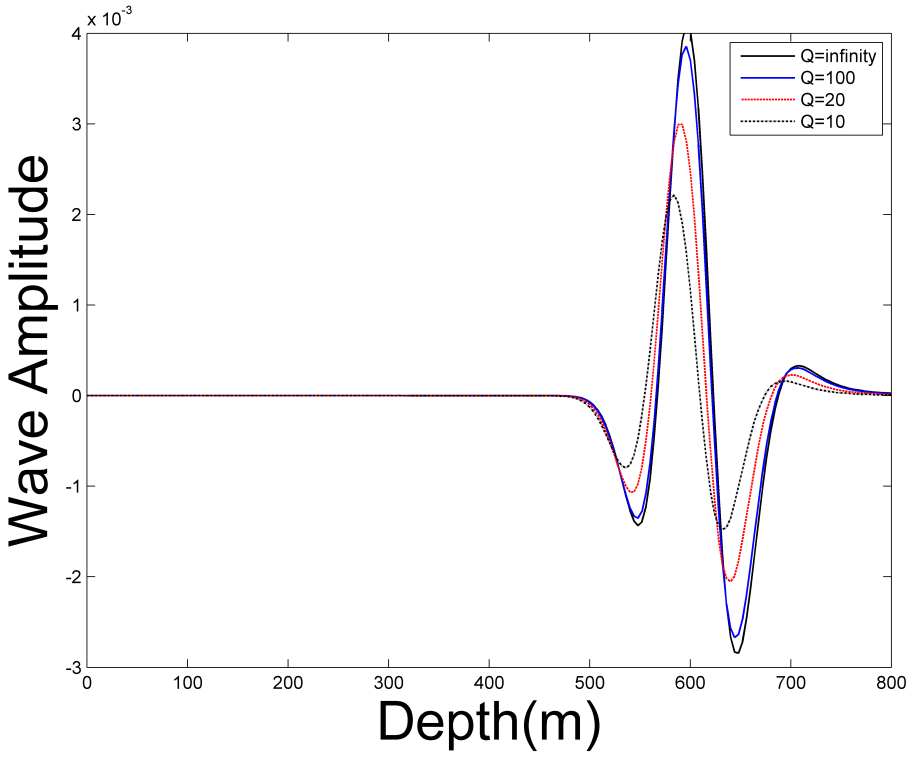

FIG. 6: Depth traces of FD showing the comparison trace number 370 of viscoacoustic VTI medium with different Q.

$$\partial_t \sigma_V = \rho V_P^2 \left[\sqrt{1+2\delta} \left[(\cos\theta\cos\varphi\partial_x - \sin\theta\partial_z)(u_x + d(z)u_x^{(1)}) \right] + \left(\frac{\tau_\varepsilon}{\tau_\sigma} \right) \left[(\cos\varphi\sin\theta\partial_x + \cos\theta\partial_z)(u_z + d(x)u_z^{(1)}) \right] - r_V \right] - (d(x)+d(z))\sigma_V - d(x)d(z)\sigma_V^{(1)}, \quad (27)$$

Similarly with VTI medium, the regularization must be considered because of high frequency instability. We construct a regularization equation based on split-field PML equation in TTI medium:

$$\partial_t \sigma_H = \rho V_P^2 \left[(1+2\varepsilon) \left[\left(\frac{\tau_\varepsilon}{\tau_\sigma} \right) \left[(\cos\theta\cos\varphi\partial_x - \sin\theta\partial_z)(u_x + d(z)u_x^{(1)}) \right] - r_H \right] + \sqrt{1+2\delta} \left[(\cos\varphi\sin\theta\partial_x + \cos\theta\partial_z)(u_z + d(x)u_z^{(1)}) \right] \right] - \left[\epsilon\rho V_P \sqrt{1+2\varepsilon} \left[\partial_t [(\cos\theta\cos\varphi\partial_x - \sin\theta\partial_z)(u_x + d(z)u_x^{(1)})] \right] \right] - (d(x)+d(z))\sigma_H - d(x)d(z)\sigma_H^{(1)}. \quad (28)$$

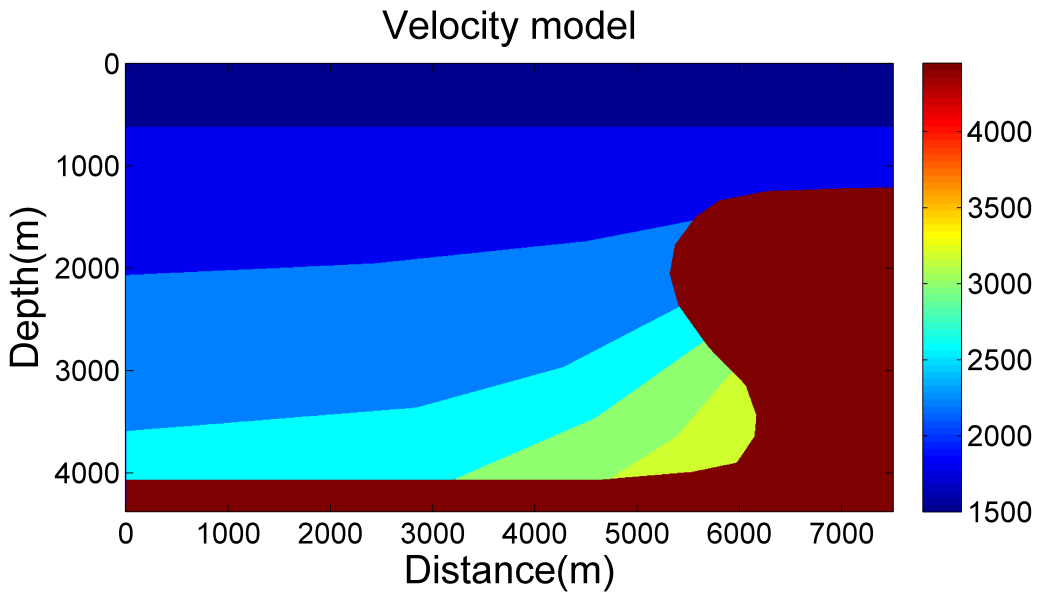

FIG. 7: P-wave velocity model.

$$\partial_t \sigma_V = \rho V_P^2 \left[\sqrt{1+2\delta} \left[(\cos\theta \cos\varphi \partial_x - \sin\theta \partial_z)(u_x + d(z) u_x^{(1)}) \right] + \left(\frac{\tau_\varepsilon}{\tau_\sigma} \right) \left[(\cos\varphi \sin\theta \partial_x + \cos\theta \partial_z)(u_z + d(x) u_z^{(1)}) \right] - r_V \right] - \left[\epsilon \rho V_P [\partial_t [(\cos\varphi \sin\theta \partial_x + \cos\theta \partial_z)(u_z + d(x) u_z^{(1)})]] \right] - (d(x) + d(z)) \sigma_V - d(x) d(z) \sigma_V^{(1)}. \tag{29}$$

where ϵ is a small positive regularization parameter.
Figure 5 shows time snapshots of viscoacoustic wave propagation in a 2D homogenous anisotropic media. The anisotropic viscoacoustic medium considered here is characterized by the constant velocity model ,$V_P = 2500m/s$, where the size of the grid is 651×651. The source is located at the center of model, and the source signature is a zero-phase Ricker wavelet with a central frequency of 25 Hz. The grid spacing in the x and z directions is 4m, and the Thomsen anisotropic parameters $\varepsilon = 0.2$ and $\delta = 0.05$. Figure 5 corresponds to an axis of symmetry tilting at 45. The compressional P wavefront is approximately ellipsoidal and the shear wave artifacts generated in an elliptic media is suppress at the source by design a small smoothly tapered circular region with $\varepsilon = \delta$ around the source.However, to avoid the numerical computation instability in TTI media, we applying the viscoacoustic equation and simply setting the shear wave velocity along the tilted symmetry axis to zero (pure P wave equation). In Figure 6 we show the effect of attenuation on amplitude and phase of a propagating seismic wave in a homogeneous anisotropic medium for different values of quality factor (Q=infinity, Q=100, Q=20 and Q=10). The attenuation affected the seismic wave energy, and the phase velocity of waves in all directions are inconsistent. There are reduced amplitude and phase shift due to dispersion. The phases do not match, and mismatch increases with the decrease of the Q value and the attenuation effect is more obvious (Figure 6). In the attenuation media the reflection wave energy decay with the increase of the depth. Therefore, the frequency bandwidth becomes narrow, the high frequency more decay and the dominant frequency move to the low frequency.

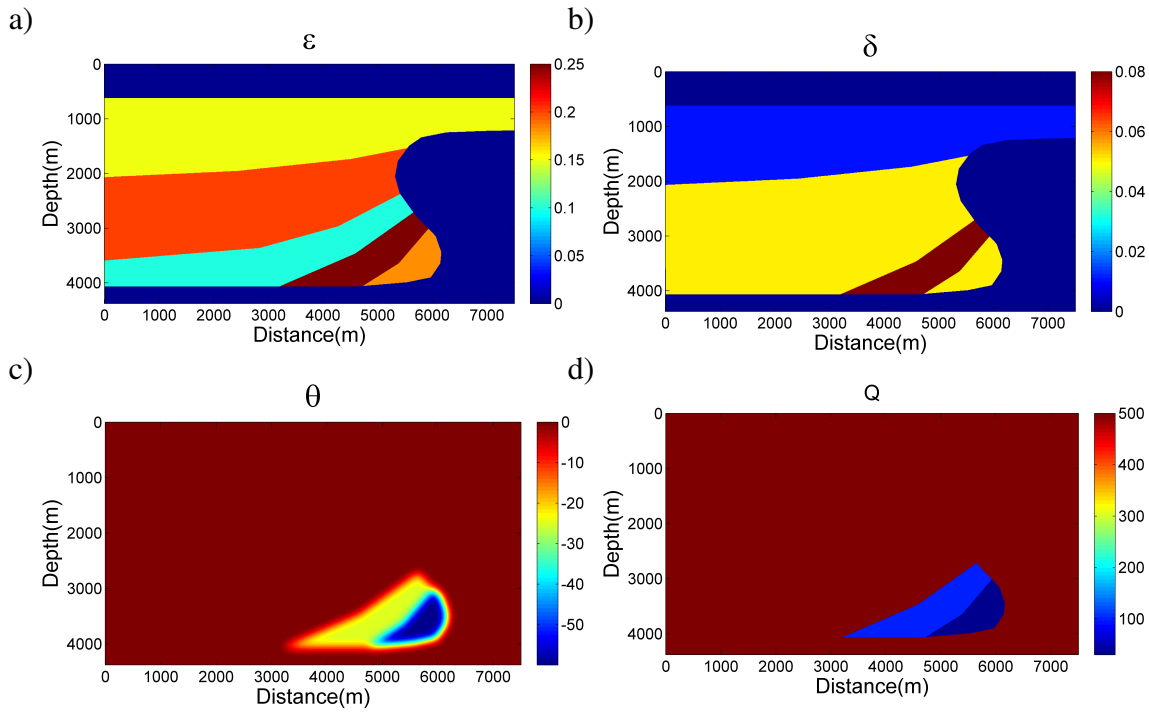

FIG. 8: Transversely isotropic velocity model. a) Thomsen's ϵ model, b) Thomsen's δ model, c)Tilted dip angle along the tilted symmetry-axis, and d)Q model.

SYNTHETIC RTM EXAMPLE

To verify the accuracy of the viscoacoustic wave equation in TTI media, the 2D data set modeled in an inhomogeneous TTI velocity model(Duveneck and Bakker, 2011) is tested (Figure 7). There are some dipping anisotropic layers in velocity model that terminating against the salt body. The Q model and three anisotropy distributions are shown in Figure 8. The rapid variation of the tilt angle affected the TTI RTM images. The model grid dimensions are 700×1200, and the grid size is 6.25 m×6.25 m. The sampling interval is 0.8 ms, and the recording length is 6 s. We use as the source a zero-phase Ricker wavelet with a center frequency of 10 Hz. To remove the effect of S-wave that generated at the source the source is located in the isotropic part of the model, i.e., $\varepsilon = \delta$. In Figure 10a snapshots of the 2D Viscoacoustic wavefield from the forward modeling simulation using the split-field PML absorbing layers are plotted. The results indicate that there is instability around in the salt area because of variation of the tilt angle. In fact, using the TI approximation and ignoring all spatial derivatives of the anisotropic symmetry axis direction leads to instabilities in some area of the model with the rapid variations in the symmetry axis direction (Duveneck and Bakker, 2011). The instability appears at the later time and can be solved with the smoothing of the model. Although smoothing the model would help in some models, but it is not useful for any models. However, Yoon et al. (2010)show that some spots of high symmetry axis gradient produce large instabilities and blows up the amplitudes of the wavefield (Figure 10a). In Figure 9a the gradient of theta is displayed. We can pick up the high gradient points by filtering the gradient of theta with a given threshold (Figure 9b). In area with instability, the anisotropy can be taken off around the selected high gradient points which set $\varepsilon = \delta$ to suppress artifacts from the source point in an anisotropic medium.

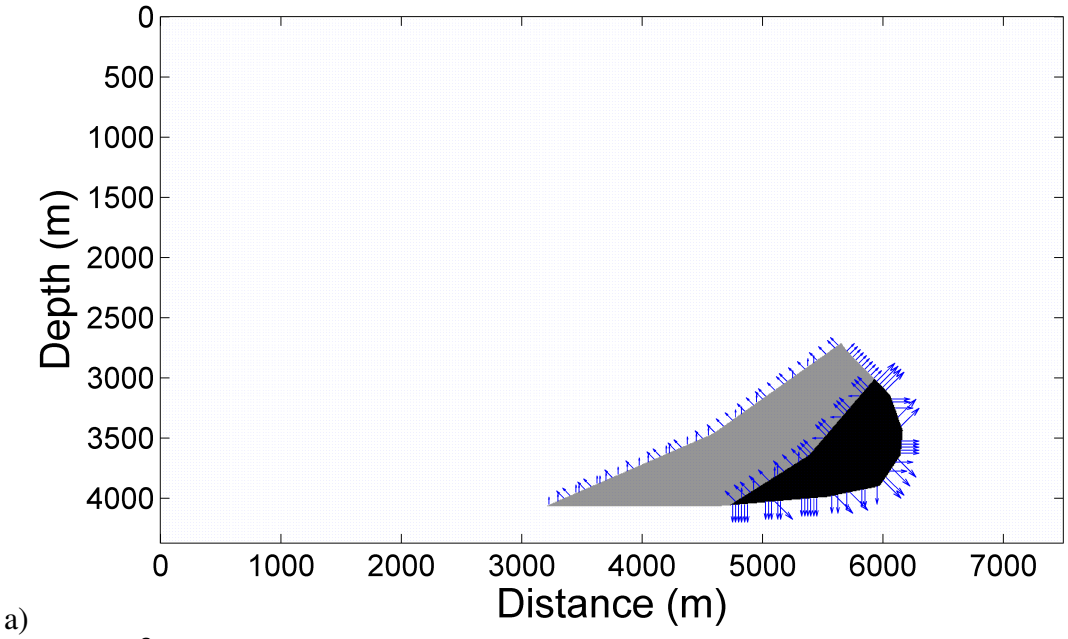

a)

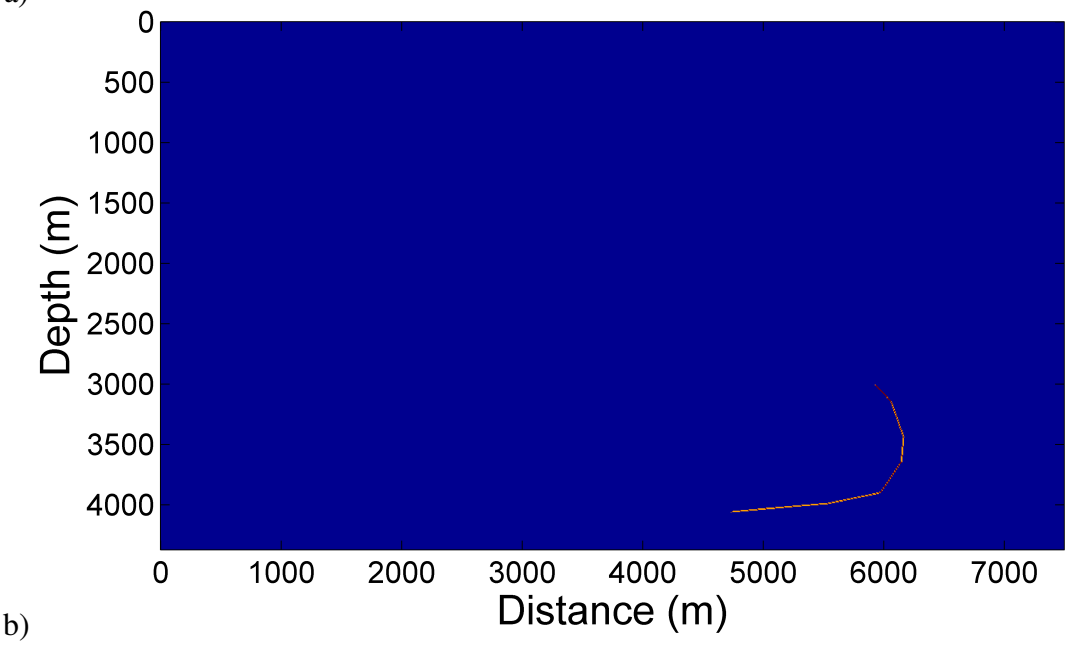

b)

FIG. 9: (a) The gradient of the tilted dip angle theta. (b) The filtered gradient by a given threshold.

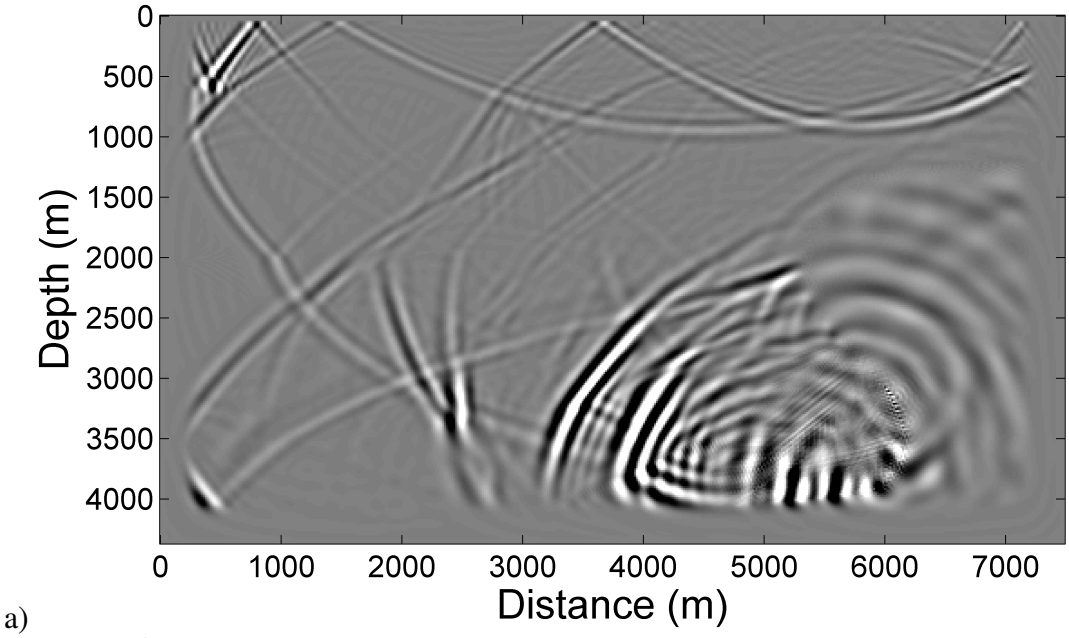

a)

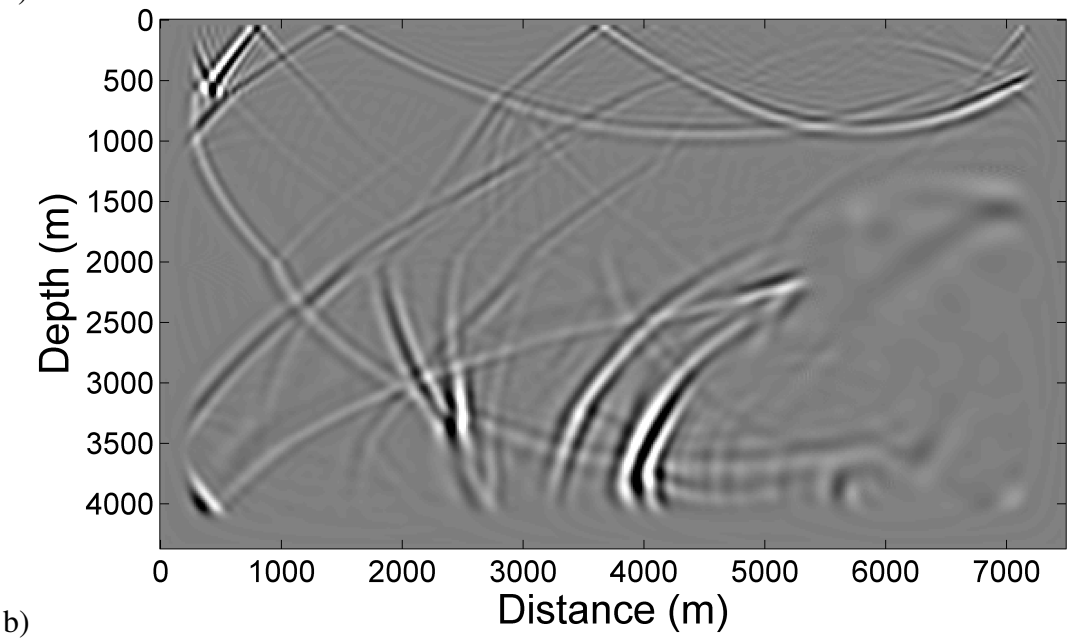

b)

FIG. 10: (a) The wavefield snapshots without anisotropic parameter equating. (d) The shot record with anisotropic parameter equating. The anisotropy effect in tilted dip angle with rapid variation is reduced by equating epsilon and delta around the high gradient points.

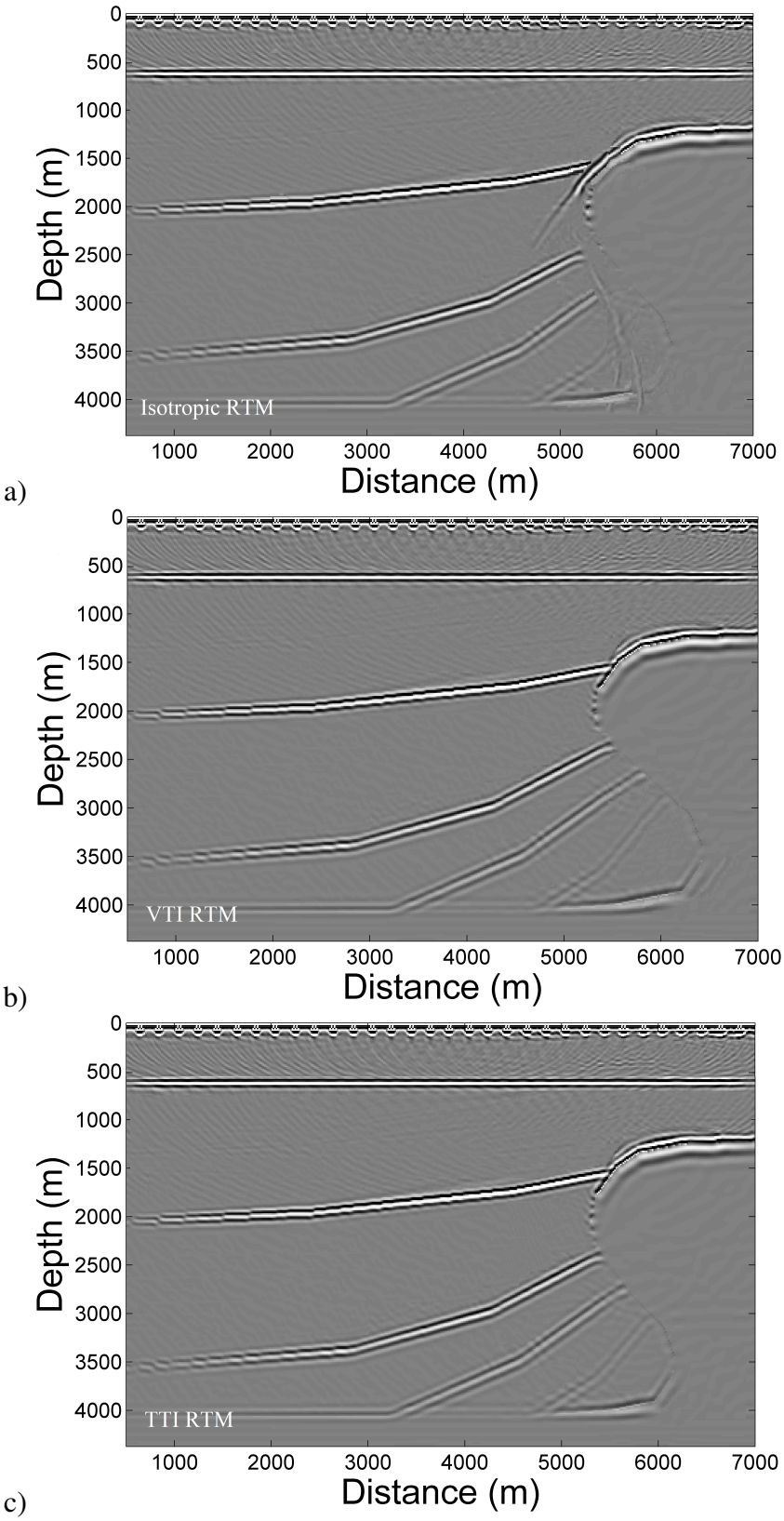

FIG. 11: Anisotropic reverse-time migration in attenuation medium. a) Isotropic revers-time migration, b) Anisotropic (VTI) Isotropic revers-time migration, and c) Anisotropic (TTI) Isotropic revers-time migration

The stable forward modeling snapshot plotted in Figure 10b.
Figure 11 shows the reverse-time migration results obtained using the split-PML field Viscoacoustic TTI equations (Figure 11c) and, for comparison, using Viscoacoustic VTI wave equations(Figure 11b) and isotropic Viscoacoustic wave equations(Figure 11a). For the VTI migration, the θ set to zero and other parameters are same with the TTI model. The imaging of dipping layers such as salt flank is affected and mispositioned in the isotropic and VTI RTM images because of the presence of anisotropy. TTI RTM for both the salt body and dipping layers that terminating against the salt body is more accurate than isotropic RTM and VTI RTM.

CONCLUSIONS

Time-domain approximate constant-Q wave propagation involving a series of standard linear solid (SLS) mechanisms is investigated. The wave equations have been extended from isotropic media to transversely isotropic (TI) media including VTI and TTI media. For imaging application, the stability condition and the artifacts of shear wave triplications have been discussed. Results show that the stable anisotropic reverse time migration is accessible by taking off anisotropy around the selected high gradient points in areas of rapid changes in the symmetry axes. The TTI RTM image is more accurate than the VTI RTM and isotropic RTM images especially in the areas with strong variations of dip angle along the tilted symmetry-axis. Furthermore, the application of anisotropic equations to 3D RTM and field data and reduce computational time remains a challenge.

ACKNOWLEDGMENTS

The authors thank the sponsors of CREWES for continued support. This work was funded by Maitacs, CREWES industrial sponsors and NSERC (Natural Science and Engineering Research Council of Canada) through the grant CRDPJ 461179-13.

REFERENCES

Alkhalifah, T., 1998, Acoustic approximations for processing in transversely isotropic media: Geophysics, **63**, 623–631.

Alkhalifah, T., 2000, An acoustic wave equation for anisotropic media: Geophysics, **67**, 1304–1325.

Blanch, J. O., Robertsson, J. O., and Symes, W. W., 1995, Modeling of a constant q: Methodology and algorithm for an efficient and opti- mally inexpensive viscoelastic technique: Geophysics, **60**, 176–184.

Carcione, J. M., Kosloff, D., and Kosloff, R., 1988, Viscoacoustic wave propagation simulation in the earth: Geophysics, **53**, 769–777.

Crampin, S., 1984, Anisotropy in exploration seismics, journal = First Break, volume = 2, pages = 19–21.

Duveneck, E., and Bakker, P. M., 2011, Stable p-wave modeling for reverse-time migration in tilted ti media: Geophysics, **76**, S65–S75.

Duveneck, E., Milcik, P., Bakker, P. M., and Perkins, C., 2008, Acoustic vti wave equa- tions and their application for anisotropic reverse-time migration: SEG Technical Program Expanded Abstracts, **27**, 2186–2190.

Fletcher, R., Du, X., and Fowler, P. J., 2008, A new pseudo-acoustic wave equation for ti media: SEG Technical Program Expanded Abstracts, **27**, 2082–2086.

Fletcher, R., Du, X., and Fowler, P. J., 2009, Reverse time migration in tilted transversely isotropic (tti) media: Geophysics, **74**, WCA179–WCA187.

Grechka, V., Zhang, L., and Rector, J. W., 2004, Shear waves in acoustic anisotropic media: Geophysics, **69**, 576–582.

Robertsson, J. O. A., Blanch, J. O., and Symes, W. W., 1994, Viscoelastic finite-difference modeling: Geophysics: Geophysics, **59**, 1444–1456.

Yoon, K., Suh, S., Ji, J., Cai, J., and Wang, B., 2010, Stability and speedup issues in tti rtm implementation: SEG Technical Program Expanded Abstracts, **29**, 3221–3225.

Zhang, H., and Zhang, Y., 2008, Reverse time migration in 3d heterogeneous tti media: SEG Technical Program Expanded Abstracts,, **27**, 2196–2200.

Zhou, H., Zhang, G., and Bloor, R., 2006a.

Zhou, H., Zhang, G., and Bloor, R., 2006b.